

Pressure Gradient Effects on Fluid Flow Through a Rotating Straight Square Duct under Magnetic field

Murshed Ahmed Ovi¹

Department of Mathematics
Bangladesh University of Engineering and
Technology
Dhaka, Bangladesh

Prodip Kumar Ghosh³

Department of Mathematics.
American International University Bangladesh
Dhaka, Bangladesh

Tajnin Rahman²

Department of Mathematics
Northern University Bangladesh
Dhaka, Bangladesh

Md Kamruzzaman⁴

Department of Mathematics
American International University Bangladesh.
Dhaka, Bangladesh.
Department of Energy and Process Engineering,
Norwegian University of Science and Technology,
Trondheim, Norway.
Email: md.kamruzzaman@ntnu.no

Abstract—This paper describes the impacts of pressure gradient in a fluid flow through a straight square duct under the magnetic field and the duct is rotated counterclockwise about the y – axis. It is an extended work of [10,11], which mainly aims at investigating pressure gradient effects with fixed magnetic (M_g) and rotation (T_r) parameter. Following two cases have been considered to analyze the flow behaviors at aspect ratio $\gamma = 1.0$ when pressure gradient (D_n) varied from 5 to 4000;

Case 1: $T_r = 100$ and $100 \leq M_g \leq 2000$.

Case 2: $T_r = 500$ and $100 \leq M_g \leq 2000$.

Steady solutions have been obtained by using spectral method. It has been observed that the fluid density increases throughout the duct with the increment of pressure gradient and magnetic field while this effect is reduced significantly by enhanced rotation. At high pressure the streamlines of secondary flow become too compact to locate vortices in that flow due to increased fluid strength. Also, Centre of axial flow distribution gets shifted towards the right wall of the duct as strong pressure gradient is noticed on the left one

Keywords—Dean number (D_n); Rotation parameter (T_r); Magnetic parameter (M_g); Spectral method.

I. INTRODUCTION

Flow through a rotating square duct in the presence of Magnetic field has magnificent usages in chemical, mechanical engineering and medical science. Fluid flow in a rotating straight duct is of interest because the secondary flows, in this case, are qualitatively similar to those in the stationary curved system (e.g.

[1]). From the beginning of 20th century, many researchers have been studying the geostrophic vortexes and ocean currents generated by the earth rotations [17]. Introduction of rotary machines into various engineering and industrial applications such as cooling systems, electric generators, gas turbines, MHD (Magneto Hydro Dynamics) pumps and flow meter, MHD steam plants, MHD separation process in metal casting etc. have drawn the concentration of researchers around the globe to look into the flow structures within these rotating system with a view to derive the corresponding characteristics [2,17]. Both coriolis and centrifugal force, resulted from the rotation of straight duct have significant impact on the flow inside it [18].

[4] found the presence of counter rotating double vortex in the secondary flow of the straight pipe while the revolution was weak. [5] studied secondary flow and showed how earth's rotation distorts the axial velocity distribution. [9] established the longitudinal roll cells as a proof to the existence of instability. Later, [13] observed the flow through a rotating straight pipe and identified the four types of flow regime in the pipe. [12, 16] conducted numerical study to identify the features of laminar flow in a rotating rectangular and square duct. Flow through a rotating square straight duct and curved duct were also analyzed numerically for both weak and strong convective inertia by [3]. Besides, [1] described the flow through a rotating straight pipe by using the Spectral method and observed the effects of rotation parameter on the square duct at different aspect ratio. [6] has simulated and studied the flow of an electricity conducting fluid

through a duct under the influence of an external magnetic field, where he placed three different obstacles (such as a circular and a square cylinder spanning over the full height of the duct and a square cylinder spanning over the half height of the duct) inside the duct. In an insulated and non-uniformly magnetized rectangular duct [15] performed computational and analytical investigations for the inertia less and inertial flows. [10] have created a numerical solution for the flow through a rotating rectangular straight duct in the presence of magnetic field and they found that flow strength weakens at high magnetic field where the center of the flow is displaced. In addition, [11] found that most axial flow moves to the centre from the wall and creates ring shape because of high magnetic parameter and large Taylor number in a rotating straight duct with large aspect ratio. [7] developed a physical mechanism regarding the formation of the secondary flow in a square duct and analyzed the momentum balance. [14] discussed the fluid flow through a rotating system under the presence of magnetic field and hall current but specified role of pressure gradient and rotation on the entire system was not clarified.

Therefore, the main aim of this study is to investigate the effects of low to moderate pressure gradient on the fluid flow in a straight square duct in the presence of Magnetic field and two different Taylor numbers.

II. GOVERNING EQUATION [11]

Let's consider laminar fluid flow of an incompressible viscous fluid through a straight duct with the steady rotation (Ω) in the presence of magnetic field. Also, assume that the length of the duct cross-section is $2a$ where a is half of the width of the duct. A Cartesian co-ordinate system (x', y', z') is considered to trace the movement of fluid particles in the duct. A constant angular velocity $\Omega = (0, -\Omega, 0)$ revolves the duct around y' - axis and the pressure gradient $-\frac{\partial p'}{\partial z'} = G$ guides fluid flow through the centerline of it. Let dimensional velocity components along x', y', z' directions are represented by u', v', w' respectively where u, v, w are used as the dimensionless ones along x, y, z direction respectively. Now the modified pressure which is a combination of gravitational and centrifugal force potentials is denoted by p' . If the fluid velocity q solves the Navier-Stokes equation, the continuity equation can be written as follows:

$$\nabla \cdot q = 0 \quad (1)$$

$$\frac{\partial q}{\partial t} + q(q \cdot \nabla) = F - \frac{1}{\rho}(\nabla \cdot p) + \nu \nabla^2 q + 2(\Omega \wedge q') \quad (2)$$

As fluid travels through the electric and magnetic field in the rotating straight square duct the equation (2) becomes,

$$\frac{\partial q}{\partial t} + q(q \cdot \nabla) = -\frac{1}{\rho}(\nabla \cdot p) + \nu \nabla^2 q + 2(\Omega \wedge q') + \frac{1}{\rho}(\mathbf{J} \wedge \mathbf{B}) \quad (3)$$

where \mathbf{J} = electric current density, \mathbf{B} = magnetic induction, Ω = angular velocity and ν = kinematic viscosity, q' = velocity vector, p = fluid pressure.

Without the presence of electric field, the generalized Ohm's law takes the following form:

$$\mathbf{J} + \frac{\omega_e \tau_e}{H_0} \mathbf{J} \wedge \mathbf{B} = \sigma'(\mu_e \mathbf{q} \wedge \mathbf{H} + \frac{1}{en_e} \nabla p_e) \quad (4)$$

where ω_e = cyclotron frequency, τ_e = electron collision, e = electric charge, n_e = number of density electron, \mathbf{H} = Magnetic field strength, μ_e = magnetic permeability, σ' = electrical conductivity.

Ignoring hall current in the equation (4) we get,

$$\mathbf{J} = \sigma'(\mu_e \mathbf{q} \wedge \mathbf{H}) [\because \omega_e \tau_e = 0 \text{ and } p_e = 0] \quad (5)$$

For boundary conditions we set $u' = v' = w' = 0$ and fully developed flow imposes all z' derivatives to zero except the pressure derivative. The duct inside is free from body force and the steady flow implies $\frac{\partial u'}{\partial t} = \frac{\partial v'}{\partial t} = \frac{\partial w'}{\partial t} = 0$. Here the axis of rotation and span of the square duct are normal to each other.

Now equations (1), (2), (3), (4) imply,

$$u' \frac{\partial u'}{\partial x'} + v' \frac{\partial u'}{\partial y'} = -\frac{1}{\rho} \frac{\partial p'}{\partial x'} + \nu \left(\frac{\partial^2 u'}{\partial x'^2} + \frac{\partial^2 u'}{\partial y'^2} \right) - 2\Omega w' - \frac{\sigma' B_0^2}{\rho} u' \quad (6)$$

$$u' \frac{\partial u'}{\partial x'} + v' \frac{\partial u'}{\partial y'} = -\frac{1}{\rho} \frac{\partial p'}{\partial y'} + \nu \left(\frac{\partial^2 v'}{\partial x'^2} + \frac{\partial^2 v'}{\partial y'^2} \right) - \frac{\sigma' B_0^2}{\rho} v' \quad (7)$$

$$u' \frac{\partial u'}{\partial x'} + v' \frac{\partial u'}{\partial y'} = -\frac{1}{\rho} \frac{\partial p'}{\partial z'} + \nu \left(\frac{\partial^2 w'}{\partial x'^2} + \frac{\partial^2 w'}{\partial y'^2} \right) + 2\Omega u' \quad (8)$$

$$\frac{\partial u'}{\partial x'} + \frac{\partial v'}{\partial y'} = 0 \quad (9)$$

Now, using the following normalized variables,

$$u' = \frac{\nu}{a} u; \quad x' = xa; \quad p' = \frac{\nu^2}{a^2} \rho p; \quad v' = \frac{\nu}{a} v; \quad y' = ya; \\ w' = \frac{\nu}{a} w; \quad z' = 0$$

where dimensional quantities are represented by the variables with prime, we obtain,

$$u \frac{\partial u}{\partial x} + v \frac{\partial u}{\partial y} = -\frac{\partial p}{\partial x} + \left(\frac{\partial^2 u}{\partial x^2} + \frac{\partial^2 u}{\partial y^2} \right) - T_r w - M_g u \quad (10)$$

$$u \frac{\partial v}{\partial x} + v \frac{\partial v}{\partial y} = -\frac{\partial p}{\partial y} + \left(\frac{\partial^2 v}{\partial x^2} + \frac{\partial^2 v}{\partial y^2} \right) - M_g v \quad (11)$$

$$u \frac{\partial w}{\partial x} + v \frac{\partial w}{\partial y} = D_n + \left(\frac{\partial^2 w}{\partial x^2} + \frac{\partial^2 w}{\partial y^2} \right) + T_r u \quad (12)$$

Here magnetic force number $M_g = \sigma' \mu_e a^2 H_0^2$, rotation parameter $T_r = 2 \left(\frac{a^2 \Omega}{v} \right)$, pressure driven parameter

$D_n = \frac{G a^3}{\rho v^2}$ and $\frac{\partial u}{\partial x} + \frac{\partial v}{\partial y} = 0$ is the continuity equation.

The boundary condition deduces $x = \pm 1, y = \pm \left(\frac{a}{a} \right) = \pm 1$ and aspect ratio $\gamma = 1$ since square cross-section is under consideration. Note that the following equations will be derived as generalized ones in terms of γ and during simulation this γ will be replaced by the value 1. Let's introduce a new variable $\bar{y} = \left(\frac{y}{a} \right)$ and assume that $u = -\left(\frac{\partial \psi}{\partial y} \right)$ and $v = \left(\frac{\partial \psi}{\partial x} \right)$ satisfy the continuity equation (9).

Therefore, the basic equation for ψ and w can be written as:

$$\begin{aligned} \frac{\partial^4 \psi}{\partial x^4} + \frac{2}{\gamma^2} \frac{\partial^4 \psi}{\partial \bar{y}^2 \partial x^2} + \frac{1}{\gamma^4} \frac{\partial^4 \psi}{\partial \bar{y}^4} = & -\frac{1}{\gamma^3} \frac{\partial \psi}{\partial \bar{y}} \frac{\partial^3 \psi}{\partial \bar{y}^2 \partial x} \\ & - \frac{1}{\gamma} \frac{\partial \psi}{\partial \bar{y}} \frac{\partial^3 \psi}{\partial x^3} + \frac{1}{\gamma^3} \frac{\partial \psi}{\partial x} \frac{\partial^3 \psi}{\partial \bar{y}^3} + \frac{1}{\gamma} \frac{\partial \psi}{\partial x} \frac{\partial^3 \psi}{\partial x^2 \partial \bar{y}} \\ & - \frac{1}{\gamma} \frac{\partial w}{\partial \bar{y}} T_r + \left(\frac{1}{\gamma^2} \frac{\partial^2 \psi}{\partial \bar{y}^2} + \frac{\partial^2 \psi}{\partial x^2} \right) M_g \end{aligned} \quad (13)$$

and

$$\begin{aligned} \frac{\partial^2 w}{\partial x^2} + \frac{1}{\gamma^2} \frac{\partial^2 w}{\partial \bar{y}^2} = & -\frac{1}{\gamma} \frac{\partial \psi}{\partial \bar{y}} \frac{\partial w}{\partial x} + \frac{1}{\gamma} \frac{\partial \psi}{\partial x} \frac{\partial w}{\partial \bar{y}} \\ & - D_n + \frac{1}{\gamma} \frac{\partial \psi}{\partial \bar{y}} T_r \end{aligned} \quad (14)$$

For ψ and w the boundary conditions are given by the following two equations,

$$\begin{aligned} w(\pm 1, \bar{y}) = w(x, \pm 1) = \psi(\pm 1, \bar{y}) = 0 \\ \left(\frac{\partial \psi}{\partial x} \right) (\pm 1, \bar{y}) = \psi(x, \pm 1) = \left(\frac{\partial \psi}{\partial \bar{y}} \right) (x, \pm 1) = 0 \end{aligned}$$

$Q' = \int_{-a}^a \int_{-a}^a w dx' dy' = v a Q$ is the dimensional total flux through the straight duct where the non-dimensional flux $Q = \int_{-1}^1 \int_{-1}^1 w dx d\bar{y}$.

III. SOLUTION METHODOLOGY [11]

Numerical methods back up the foundation of this work. The Spectral method produces the solution and polynomial functions generated expansion creates a steady or un-steady solution. Assuming the flow along axial direction as symmetric one and using series of Chebyshev polynomial in the x and \bar{y} directions

expansion functions $\varphi_n(x)$ and $\psi_n(x)$ are expressed as

$$\varphi_n(x) = (1 - x^2) T_n(x) \quad (15)$$

$$\psi_n(x) = (1 - x^2)^2 T_n(x) \quad (16)$$

where n-th order first kind Chebyshev polynomial $T_n(x) = \cos(n \cos^{-1}(x))$.

Now using $\varphi_n(x)$ and $\psi_n(x)$, the expansions of $w(x, \bar{y})$ and $\psi(x, \bar{y})$ take the following forms:

$$w(x, \bar{y}) = \sum_{m=0}^M \sum_{n=0}^N w_{mn} \varphi_m(x) \varphi_n(\bar{y}) \quad (17)$$

$$\psi(x, \bar{y}) = \sum_{m=0}^M \sum_{n=0}^N \psi_{mn} \psi_m(x) \psi_n(\bar{y}) \quad (18)$$

where truncation numbers along x and \bar{y} directions are denoted by M and N respectively. The application of the Collocation method [8] in x and \bar{y} directions produce a set of nonlinear differential equations involving w_{mn} and ψ_{mn} . Let's take (x_i, \bar{y}_j) as collocation points where,

$$x_i = \cos \left[\pi \left(1 - \frac{i}{M+2} \right) \right], (i = 1, 2, \dots, M+1) \quad (19)$$

$$\bar{y}_j = \cos \left[\pi \left(1 - \frac{j}{N+2} \right) \right], (j = 1, 2, \dots, N+1) \quad (20)$$

and the extended non-linear differential equations are,

$$(A_1 + B_1 + C_1)w = N_1(w_{mn}, \psi_{mn}) \quad (21)$$

$$(A_2 + B_2 + C_2)\psi = N_2(w_{mn}, \psi_{mn}) \quad (22)$$

In the above two equations (21) and (22); A_1, B_1, C_1 and A_2, B_2, C_2 are $(M+1)(N+1)$ dimensional square matrices, $w = (W_{00} \dots W_{M0} \dots W_{0N} \dots W_{MN})$, $\psi = (\psi_{00} \dots \psi_{M0} \dots \psi_{0N} \dots \psi_{MN})$ and N_1, N_2 are the non-linear operators. Now the following non-linear algebraic equations are solved by the Newton-Raphson method.

$$w^{(p+1)} = C_1^{-1} N_1(w_{mn}^{(p)}, \psi_{mn}^{(p)}) \quad (23)$$

$$\psi^{(p+1)} = C_2^{-1} N_2(w_{mn}^{(p)}, \psi_{mn}^{(p)}) \quad (24)$$

where p has been used for iteration number. The usage of arc-length method eliminates the complexity near the inflection points of steady solution. Using 'S' as a symbol of arc-length the arc-length equation becomes,

$$\sum_{m=0}^M \sum_{n=0}^N \left[\left(\frac{dw_{mn}}{ds} \right)^2 + \left(\frac{d\psi_{mn}}{ds} \right)^2 \right] = 1 \quad (25)$$

The Newton-Raphson method uses equations (23) and (24) to solve the above equation. Beginning with

s , an initial guess is made at $s + \Delta s$ by dint of following two equations.

$$w_{mn}(s + \Delta s) = w_{mn}(s) + \frac{dw_{mn}(s)}{ds} \Delta s \quad (26)$$

$$\psi_{mn}(s + \Delta s) = \psi_{mn}(s) + \frac{d\psi_{mn}(s)}{ds} \Delta s \quad (27)$$

An iteration is performed to generate a correct solution at $s + \Delta s$. Now for the convergence let's take sufficiently small ϵ_p ($\epsilon_p < 10^{-8}$) where,

$$\epsilon_p = \sum_{m=0}^M \sum_{n=0}^N \left[(w_{mn}^{(p+1)} - w_{mn}^{(p)})^2 + (\psi_{mn}^{(p+1)} - \psi_{mn}^{(p)})^2 \right] \quad (28)$$

IV. RESULT AND DISCUSSIONS

In this study our considerable situation includes the observation of flow structures of the laminar flow of a pressurized incompressible viscous fluid through a magnetized straight square duct which is rotating at a constant angular velocity Ω . Without rotation, there would have been a unidirectional velocity field. To explore the impact of pressure gradient on the flow, we have the pressure parameter D_n (Dean Number) changed continuously while magnetic field parameter M_g , rotation parameter T_r (Taylor Number) and aspect ratio remained constant. That's why the following two cases are taken into account where both had an aspect ratio $\gamma = 1$.

Case 1: $T_r = 100$ and $M_g = 100, 500, 1000, 2000$.

Case 2: $T_r = 500$ and $M_g = 100, 500, 1000, 2000$.

Coriolis force, a resultant of duct rotation is the generator of secondary flow for both the cases [3]. Two types of secondary flow are expected, one is in the anti-clockwise direction ($\psi \geq 0$) and the other is following the clockwise direction ($\psi < 0$). Also, the contour plotting of axial flow distribution through the square duct under the accounted cases need to be visualized for better anatomy.

Case 1

Firstly, we investigate the streamlines of secondary flow and contour plotting of axial flow. For the following four figures at $T_r = 100$ and streamlines of the secondary flow is at the top and contour plot of axial flow is at the bottom. At the top part, solid lines represent the anti-clockwise secondary flow whereas the dotted ones are for the clockwise streamlines.

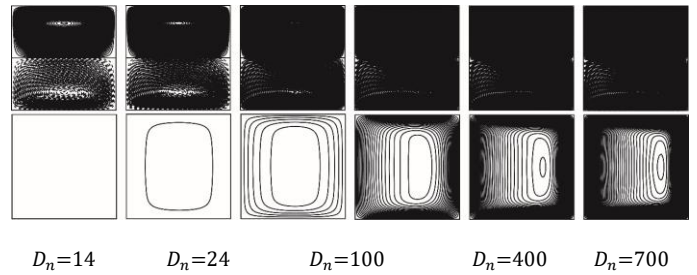


Figure 1. Streamlines of secondary flow (top) and Contour plotting of Axial flow (bottom) for $M_g = 100$ and $T_r = 100$ under the specified D_n (Placed at the very bottom).

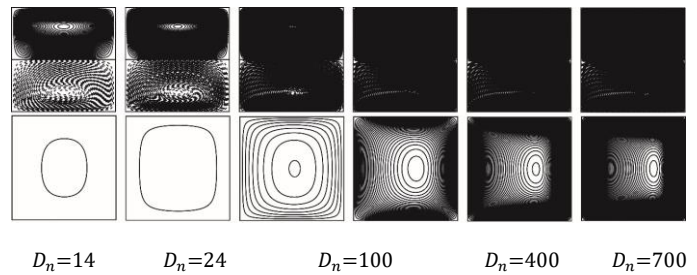


Figure 2. Streamlines of secondary flow (top) and Contour plotting of Axial flow (bottom) for $M_g = 500$ and $T_r = 100$ under the specified D_n (Placed at the very bottom).

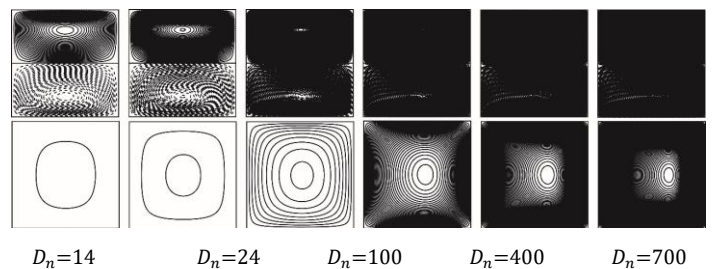


Figure 3. Streamlines of secondary flow (top) and Contour plotting of Axial flow (bottom) for $M_g = 1000$ and $T_r = 100$ under the specified D_n (Placed at the very bottom)

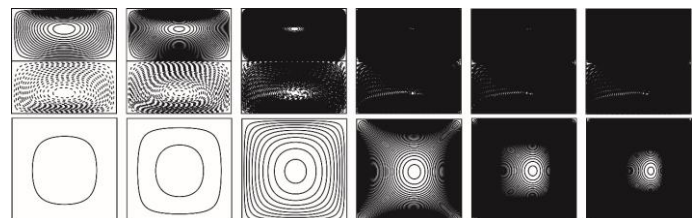


Figure 4. Streamlines of secondary flow (top) and Contour plotting of Axial flow (bottom) for $M_g = 2000$ and $T_r = 100$ under the specified D_n (Placed at the very bottom).

From each of the above figures (Figure 1 - Figure 4) we notice the existence of two counter rotating vortices in the secondary flow at lower pressure and they start disappearing at higher pressure ($D_n > 100$). Also, the center of axial flow distribution is forced towards the right wall of the duct and it doesn't get distorted from its circular ring shape. Gradual increment of darkness with pressure in each figure bears a sign of enhanced fluid density i.e. flow strength. To justify this, allow us to investigate the flux variations as the pressure changes.

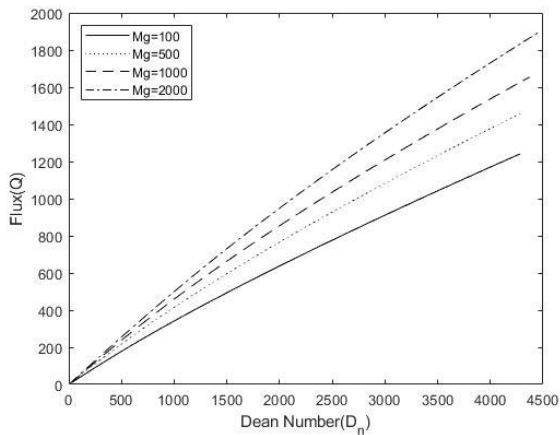


Figure 5. Steady solution curve for $\gamma = 1, T_r = 100, M_g = 100, 500, 1000, 1500$ and $0 \leq D_n \leq 4500$.

Case 2

Also, for this case the following four graphs have same pattern as in Case 1 i.e. streamlines of secondary flow is at the top and contour plot of axial flow is at the bottom. For this case rotation parameter $T_r = 500$ has been used.

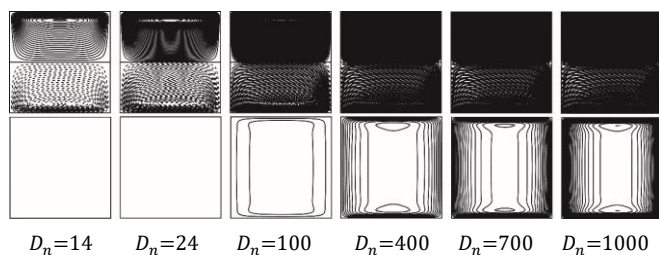


Figure 6. Streamlines of secondary flow (top) and Contour plotting of Axial flow (bottom) for $M_g = 100$ and $T_r = 500$ with specified D_n (Placed at the very bottom).

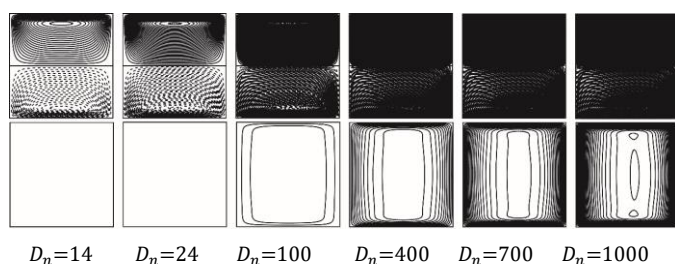


Figure 7. Streamlines of secondary flow (top) and Contour plotting of Axial flow (bottom) for $M_g = 500$ and $T_r = 500$ with specified D_n (Placed at the very bottom).

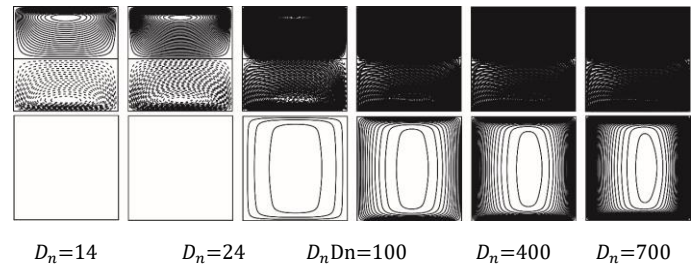


Figure 8. Streamlines of secondary flow (top) and Contour plotting of Axial flow (bottom) for $M_g = 1000$ and $T_r = 500$ under with specified D_n (Placed at the very bottom).

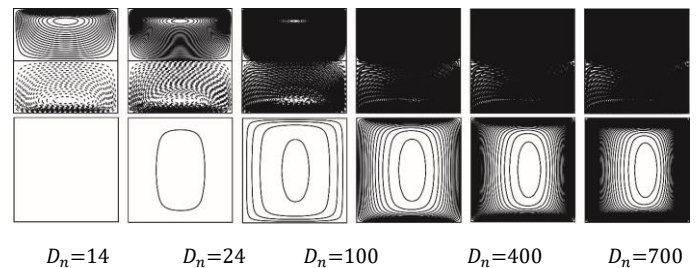


Figure 9. Streamlines of secondary flow (top) and Contour plotting of Axial flow (bottom) for $M_g = 2000$ and $T_r = 500$ with specified D_n (Placed at the very bottom).

The four figures (Figure 6 - Figure 9) also have shown that for lower pressure in the plane which is normal to the axis of rotation, the stream lines of the secondary flow contain two counter rotating vortices and the increased pressure moves the center of these vortices in the vicinity of the upper and lower wall. When the pressure increases significantly ($D_n > 100$) streamlines of secondary flow become too dense to locate any flow pattern. From the contour plots generated for $M_g = 100$ and 500 , distorted center of axial flow distribution is noticed as the pressure increases whereas other two cases (for $M_g = 1000$ and 2000) maintain circular ring shape at the center. Besides, in the above four figures (Figure 6 - Figure 9) center of axial flow is shifted towards the right wall of the duct as strong pressure gradient is dominant on the left wall. For $T_r = 500$, in all the graphs darkness in the streamlines plotting and contour plotting increases but at a lower rate than the Case 1. This result indicates lower fluid strength than the previous case as pressure changes. And this

statement is backed by the following graph of Dean Number versus flux when rotation parameter is 500.

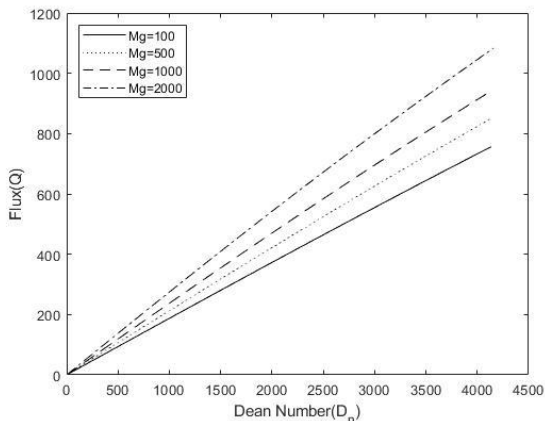


Figure 10. Steady solution curve for $\gamma = 1, T_r = 500, M_g = 100, 500, 1000, 1500$ and $0 \leq D_n \leq 4500$.

Figure 10 explains that the flux is increasing with pressure but if we compare Figure 5 and Figure 10 we see that fluid strength is lower in the second case. To find the reason behind this change we need to identify the role of rotation and magnetic field. In order to know the influence of magnetic field the following graph is drawn by keeping rotation and pressure fixed allowing magnetic parameter to change.

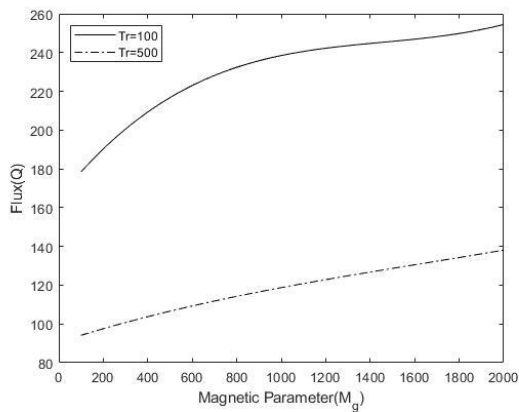


Figure 11. Change of Flux with M_g where $D_n = 500$.

The Figure 11 shows that for the same rotation, as the magnetic parameter increases so does the flux. Now to know the impact of rotation, analyzing Figure 11 it becomes vivid that flux gets reduced by the increment of rotation. For instance, let $M_g = 100$, and pressure $D_n = 500$ then for $T_r = 100$ the flux value is 1.7845×10^2 whereas for $T_r = 500$ it becomes 94.13. So, it can be concluded that enhancement of rotation is responsible for the reduction of streamline density in the second case. With a specific magnetic field and a significantly large pressure, if we increase the number of rotations in the square duct the flux will decrease, the darkness in the figures (Figure 1- Figure 4, Figure

6- Figure 9) of stream lines will get lesser and the vortices will be more traceable. This above statement can be supported by the data and figures in [10,11] Furthermore, to verify, whether the obtained characteristics remain same for higher pressure we have generated more contour plot of axial flow profile only because the streamlines get too dense to identify any flow pattern for the secondary flow. The axial velocity distribution analysis has been done for the previous two cases with higher pressure $D_n = 1500, 2000, 2500, 3000, 3500, 4000$. First take higher pressure added Case 1 into consideration.

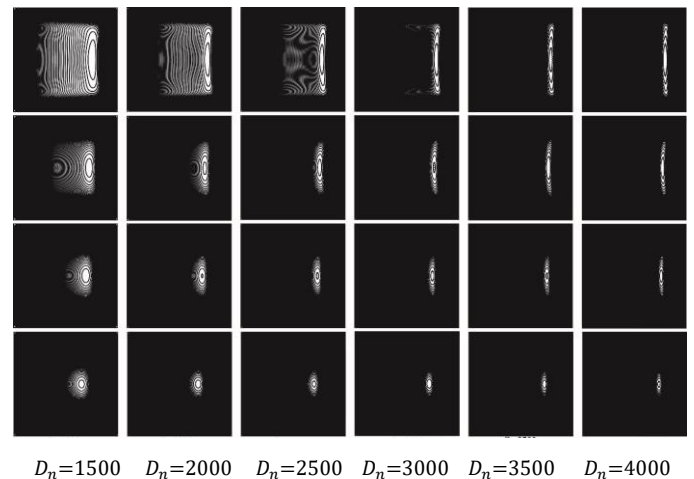


Figure 12. Axial flow distribution from the top for $M_g = 100, 500, 1000, 2000$ respectively with $T_r = 100$ and specified D_n (Placed at the very bottom).

As in Case 1 the center here is still in extant with circular ring shape and moved in the direction of the right wall by these extreme pressures. And also, the fluid strength is increasing gradually with pressure. Now for the Case 2 with higher pressure let's observe the following figure

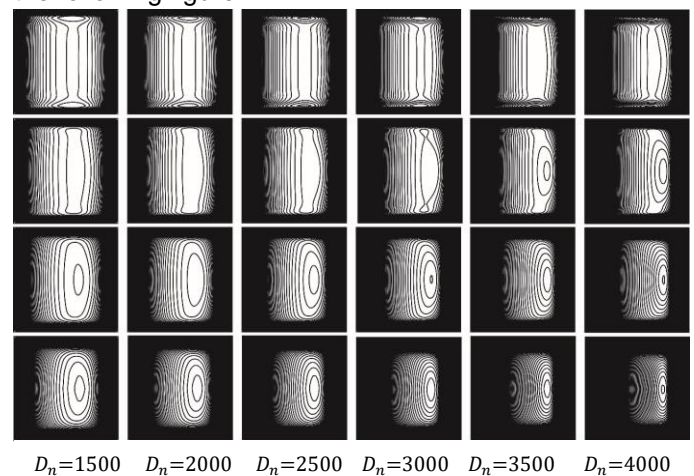


Figure 13. Axial flow distribution from the top for $M_g = 100, 500, 1000, 2000$ respectively with $T_r = 500$ and specified D_n (Placed at the very bottom).

At these immense pressures the distorted center is yet visible for $M_g = 100, 500$ as similar happened in Case 2 analysis and it gets closed to the right wall by the pressure. Fluid density also increases.

V. CONCLUSION

A numerical study about the impact of pressure gradient on the incompressible fluid flow passing through a magnetized rotating straight square duct has been conducted. The steady solution was obtained for every considered case. At the straight square duct two counter rotating vortices exist in the secondary flow when the pressure is low. The flow strength through the duct increases with pressure enhancement. With significant increment in pressure streamlines become so integrated that vortices in the secondary flow remain unidentified. Also, Magnetic field stimulates the flux in the duct. The center of axial flow distribution is moved near the right wall of the duct as the pressure gradient increases. The impact of pressure gradient on the flow can be reduced by increasing the rotation.

VI. ACKNOWLEDGMENT

Thanks, must go to Professor Dr Mahmud Alam, Mathematics Department, Khulna University for his stimulating discussion on this topic.

REFERENCES

- [1] Alam M.M., Begum, D and Yamamoto K., "Flow through a rotating straight pipe with large aspect ratio," *J. Energy Heat and Mass Transfer*, Vol 9(2):153, 2007.
- [2] Al-Khawaja M. and Selmi M., "Finite difference solutions of MFM square duct flow with heat transfer using MatLab program," *Sciyo.Com*, 5:365, 2010.
- [3] Baekt J. H. and Ko C. H., "Numerical Flow Analysis in a Rotating Square Duct and a Rotating Curved-Duct," *Int. J. Rot. Mech.* Vol. 6(1), pp. 1-9, 2000
- [4] Barua S.N., "Secondary flow in a rotating straight pipe," *Proc. Roy. Soc. London Series A. Math and Phys. Sci.*, Vol 21:227(1168), pp.133-139, 1954.
- [5] Benton G.S. and Baltimore M. D., "The effect of the earth's rotation on laminar flow in pipes," *J. Appl.Mech.*, Vol. 23, pp.123-127, 1956.
- [6] Dousset, Vincent. "Numerical simulations of MHD flows past obstacles in a duct under externally applied magnetic field." PhD diss., Coventry University, 2009.
- [7] Dai Y. J. and Xu C. X., "Wall pressure and secondary-flow origination in a square duct," *Vol.2:31(8):085104*, 2019.
- [8] Gottlieb D. and Orszag S., "Numerical analysis of spectral methods: Theory and Applications," *Soc. Ind. App.Math.*, CBMS_NSF Regional Conference Series in Applied Mathematics, 1977.
- [9] Hart J. E., "Instability and secondary motion in a rotating channel flow," *45(2):341-51*, 1971.
- [10] Kamruzzaman, M. Wahiduzzaman, M, Alam, MM, Ferdows M, Hossain M, & Quadir R.A., "Numerical solutions of fluid flow through a rotating rectangular straight duct with magnetic field," *Int. J. Mech. Eng. (IJME)*, Vol. 2(2), pp 69-86, 2013.
- [11] Kamruzzaman M, Wahiduzzaman M, Alam MM, Djenidi L., "The effects of magnetic field on the fluid flow through a rotating straight duct with large aspect ratio," *Proc. Eng.*, Vol,1: 56, 239-44, 2013.
- [12] Khesghi H. S. and, Scriven L. E., "Viscous flow through a rotating square channel," *Phys.Fluids A: Fluid Dynamics*, 28(10):2968-79, 1985.
- [13] Lei U. and Hsu C.H., "Flow through rotating straight pipes," *Phys. Fluids*, 2(1), pp.63-73, 1990.
- [14] Lima K. F. and Alam M. M., "Fluid flow through a straight pipe in a rotating system with magnetic field acting along center line having hall current," *AIP Con. Proc.* Vol. 2121, No. 1, p. 040003, 2019.
- [15] Moreau R, Smolentsev S, Cuevas S., "MHD flow in an insulating rectangular duct under a non-uniform magnetic field," *PMC Phys. B* Vol. 1:3(1):3, 2010.
- [16] Speziale C. G., "Numerical study of viscous flow in rotating rectangular ducts," *J. Fluid. Mech.*, 122:251-71, 1982.
- [17] Yang W. J., Fann S and Kim J H, "Heat and fluid flow inside rotating channels." *App. Mech. Rev.*, Vol. 7(8), pp. 367-396, 1994.
- [18] Zhang J, Zhang B, and Jü J., "Fluid flow in a rotating curved rectangular duct", *Int. J. Heat and Fluid Flow*, Vol. 1:22(6), pp.583-592, 2001